Interannual Rainfall Variability over the South American Altiplano

René D. Garreaud and Patricio Aceituno

Department of Geophysics, Universidad de Chile, Santiago, Chile

(Manuscript received 4 May 2000, in final form 1 September 2000)

ABSTRACT

Summertime (December–February) precipitation is virtually the only water resource over the South American Altiplano, a semiarid, high-level plateau entrenched in the central Andes. On the interannual timescale, Altiplano rainfall exhibits pronounced fluctuations between drought and very wet conditions, with subsequent impacts on agriculture and hydrology. In this work, the large-scale patterns of convective cloudiness and circulation associated with interannual variability of the summer rainfall over this region are investigated using a regression analysis between relevant atmospheric fields (NCEP–NCAR reanalysis, outgoing longwave radiation) and an index of convection over the Altiplano.

It is found that the seasonal-mean, large-scale zonal flow over the central Andes is directly related with the number of days with easterly flow within the season, that, in turn, favor the occurrence of summertime deep convection on the Altiplano by transporting moist air from the interior of the continent. Consequently, interannual variability of the seasonal-mean zonal wind explains nearly half of the variance of summertime convection over the Altiplano through an easterly/wet–westerly/dry pattern. The circulation anomalies are in geostrophic balance with changes in the meridional baroclinicity at the southern border of the tropical belt. Thus, a previously documented relationship between El Niño–Southern Oscillation (ENSO) phenomenon and interannual rainfall variability over the Altiplano is explained by the generalized warming (cooling) of the tropical troposphere during the negative (positive) phase of ENSO and the associated strengthening (weakening) of the westerlies over the central Andes.

1. Introduction

Several issues have motivated a growing interest on the rainfall variability over the South American Altiplano, a high level (~3800 m) plateau situated in the central Andes between 15° and 21°S. First, summertime rainfall is virtually the only water resource for inhabitants and agriculture over this semi-arid region, although intense storms (as those during January 2000) can produce local flooding and trigger flash floods over the slopes of the Andes. Furthermore, a fraction of the summer rainfall and snowmelting represent the only recharge of the underground water system of the Altiplano and the dry western slope of the Andes, controlling the regional hydrology on very long timescales. Second, surface heating and deep moist convection release large amounts of energy into the middle and upper troposphere over the central Andes linking rainfall variability on the Altiplano with circulation and rainfall anomalies over the rest of South America (e.g., Zhou and Lau 1998). Finally, paleoclimatic records obtained from dry lakes and glaciers on the Altiplano require a better knowledge of present climate variability in order to unveil past environmental conditions and climate variability in the region (e.g., Thompson et al. 1998).

Mean atmospheric conditions over the Altiplano (e.g., Schwerdtfeger 1976; Aceituno 1998; see also Fig. 1) feature a strong gradient between very dry and stable conditions in the southwestern sector (bordered by the southern Peru–northern Chile desert) and more humid conditions in the northeastern sector (immediately to the west of the Amazon basin). Altiplano rainfall also exhibits a pronounced annual cycle closely related to seasonal changes of the atmospheric circulation (e.g., Aceituno 1998). Over 60% of the annual precipitation is concentrated in the austral summer [December–February (DJF)] in the form of intense convective rainstorms along the plateau (e.g., Garreaud 2000), when easterly flow prevails over the central Andes allowing moisture transport from the interior of the continent up to the Altiplano. Superimposed on the mean summertime conditions, rainy days tends to cluster in ''rainy episodes,'' lasting from 1 to 2 weeks, interrupted by dry periods of similar length. Basin-scale conditions during these episodes are described in Garreaud (1999, 2000), while their attending large-scale circulation anomalies are described, among others, by Fuenzalida and Rutllant (1987), Aceituno and Montecinos (1993), Vuille et al. (1998), Lenters and Cook (1999), and Garreaud (1999).

Corresponding author address: Dr. René D. Garreaud, Department of Geophysics, Universidad de Chile, Blanco Encalada 2085, Santiago, Chile.
E-mail: rgarreau@dgf.uchile.cl

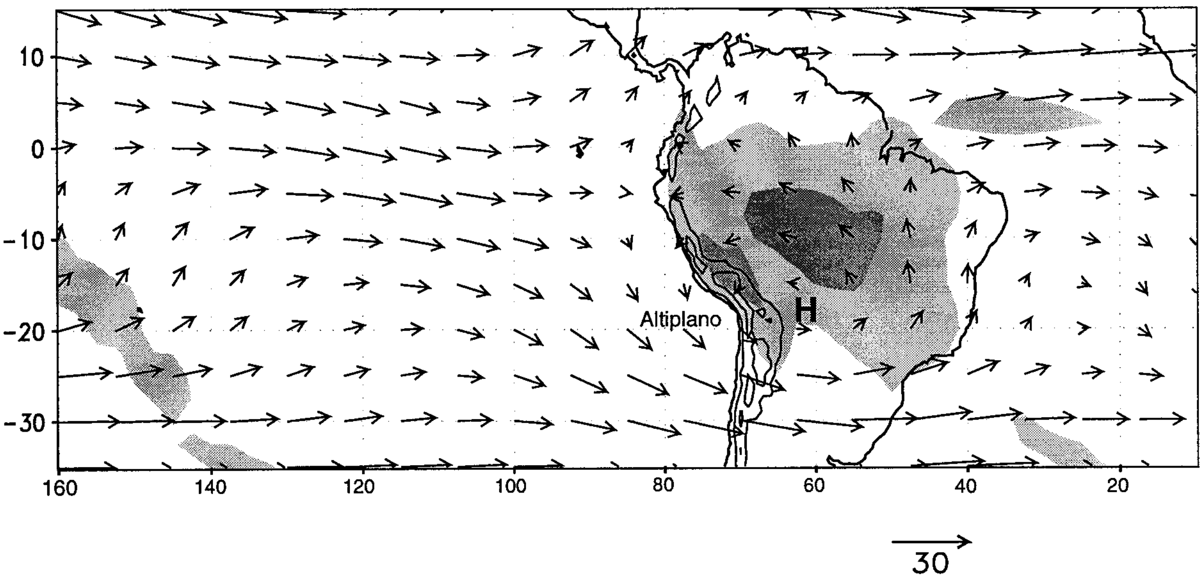

FIG. 1. Climatological summertime mean winds at the 200-hPa level and outgoing longwave radiation (OLR). Wind vector reference at the bottom is 30 m s^{-1}. Light and medium shading indicates OLR less than 235 and 215 W m^{-2}, respectively. Thin solid contours indicate terrain elevation in excess of 2000 and 4000 m. Center of the Bolivian High is indicated by a letter H.

Consistent with its transitional character in time and space, rainfall over the Altiplano is highly sensitive to large-scale circulation anomalies. On the interannual timescale, surface-based observations indicate alternating of drought and very wet summer condition (e.g., Ronchail 1998). For instance, the area-average summertime rainfall[1] shown in Fig. 2 ranges from 50 to +500 mm season^{-1} and pronounced fluctuations are also observed in the time series of the summertime increment of the level of Lake Titicaca (an integrated index of summertime rainfall over the northern Altiplano).

Several studies have shown that a significant fraction of the interannual variability of precipitation on the Altiplano is related to the El Niño–Southern Oscillation (ENSO) phenomenon (Thompson et al. 1984; Francou and Pizarro 1985; Aceituno 1988; Aceituno and Garreaud 1995; Ronchail 1995, 1998; Lenters and Cook 1999; Vuille 1999). Based on different estimates of summertime precipitation (rainfall station data, Titicaca lake level, snow accumulation) and statistical techniques these studies document a tendency for wet conditions during the cold ENSO phase (La Niña years) and dry conditions during the warm ENSO phase (El Niño years). As evident in Fig. 2, however, neither all rainiest/driest summers occur during extreme ENSO years, nor all El Niño/La Niña years are associated with extreme rainfall anomalies (see also Aceituno and Garreaud 1995; Vuille 1999). The weakness of the relationship between ENSO and summertime rainfall could be at least partially caused by the large spatial and intraseasonal variability of the precipitation over the Altiplano. For instance, recent work by Vuille et al. (2000) shows that ENSO-related rainfall anomalies are much more pronounced and statistically significant over the western sector compared with those over the northeastern sector of the Altiplano. In any case, the physical link between global-scale circulation anomalies (e.g., ENSO) and Altiplano rainfall anomalies is unclear.

In the present work we investigate the interannual rainfall variability over the Altiplano in a more general context, without focusing a priori on the ENSO signal. Specifically, we aim to characterize the year-to-year fluctuations of the summertime rainfall over the central Andes and their relationship with rainfall changes elsewhere (e.g., over the rest of South America) and large-scale circulation anomalies. Only after this step we investigate whether or not the ENSO signal projects upon the anomaly fields associated with Altiplano rainfall variability. Satellite measurements of outgoing longwave radiation (OLR) are used as a proxy of convective rainfall over the Altiplano. Comparison of OLR with other estimates of precipitation and a description of the datasets used in this study are presented in section 2. Considering that year-to-year variability is ultimately produced by changes in the number or intensity of rainfall episodes within the summer season, we first review the large-scale circulation patterns associated with intraseasonal rainfall variability on the Altiplano (section 3). In section 4 we document the seasonal-mean, large-scale

[1] The rainfall data in Fig. 2 must be taken with caution, because it is based on a small and variable number of stations (2–4) with gaps in its original records. Furthermore, the 5° × 5° lat–long rainfall average is a large simplification of the real conditions over the Altiplano, possibly biased by the more humid conditions in the northeast sector of the basin. The convective and episodic nature of the rainfall over the Altiplano also substract representativeness to area average rainfall estimated from a reduced number of stations.

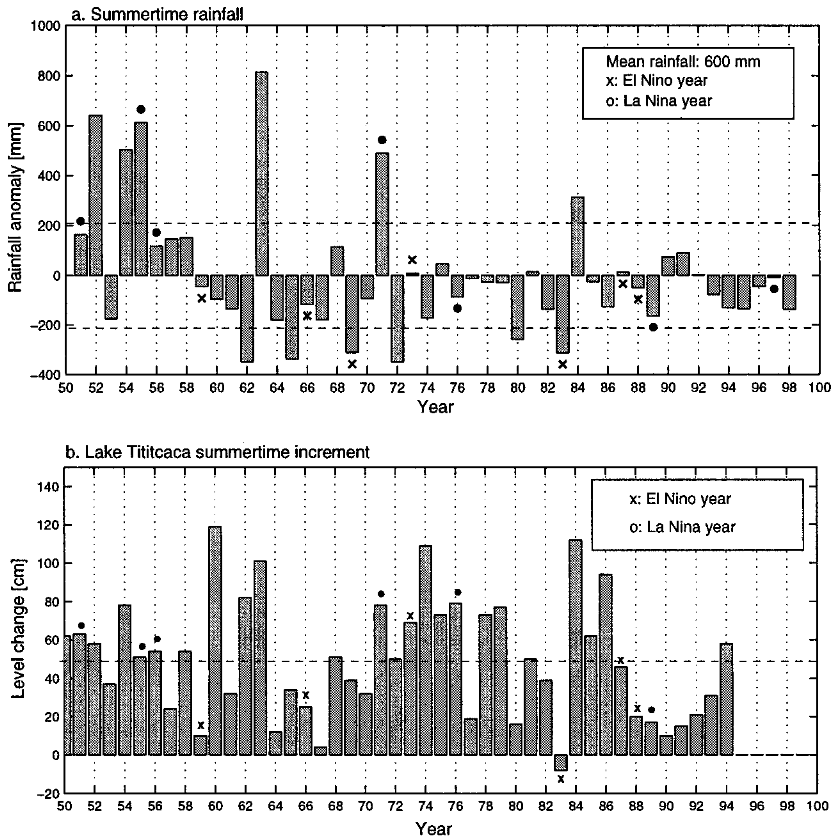

FIG. 2. (a) Summer rainfall anomalies on a 5° × 5° grid box centered at 17.5°S 67.5°W. The year mark the Jan–Feb part of the respective austral summer. Monthly values obtained from gridded rainfall data available from NASA Goddard Institute for Spatial Studies (Dai et al. 1997). Gridded data was synthesized from original station records on this region compiled at the Climate Research Unit, University of East Anglia, UK (Hulme 1992). (b) Variation of the level of Lake Titicaca (northern Altiplano) measured at Puno (15.9°S, 70.0°W, 3800 m) between 1 Dec and 28 Feb (summertime increment). In both panels cross (filled circle) indicates El Niño (La Niña) conditions during the corresponding austral summer.

circulation, and convection anomalies related to summertime rainfall variability and their impact upon intraseasonal episodes. A physical link between global-scale phenomena (including ENSO) and interannual rainfall variability over the Altiplano emerges from this analysis. A summary of our results is presented in section 5.

2. Datasets and methodology

Daily and monthly outgoing longwave radiation (OLR) on a 2.5° × 2.5° grid box centered at 17.5°S, 70°W was used as an index of the convective precipitation over the Altiplano (CI). Original OLR fields on a 2.5° lat–long grid are available from December 1974 [see Liebmann and Smith (1996) for further details on this dataset] and they have been widely used as a proxy of rainfall over tropical and subtropical regions (e.g., Meisner and Arkin 1987). Despite its coarse spatial resolution and lack of direct relationship with the amount of rain, interannual fluctuations of CI agree well with other rainfall estimates over the Altiplano (Fig. 3). In interpreting subsequent results it is worth keeping in mind that the linear dependence between summer mean CI and summer rainfall (station data) is, roughly, $\delta(\text{Rain})/\delta(\text{-CI}) \sim 100$ mm $(10 \text{ W m}^{-2})^{-1}$ (Fig. 3a).

The large-scale tropospheric circulation was characterized using the National Centers for Environmental Prediction–National Center for Atmospheric Research (NCEP–NCAR) reanalysis fields (Kalnay et al. 1996) on global 2.5° lat–long grids available since 1958. Because the enhanced amount of assimilated data (including satellite wind data since 1979) the reanalysis are thought to realistically portray the atmospheric circulation on synoptic, seasonal, and interannual scales, even in regions with sparse conventional observations. Over the Altiplano, reanalysis data underestimate the amplitude of the *mean* diurnal cycle of several variables (Aceituno and Montecinos 2000) but they do capture most of the intraseasonal variability in moisture and midlevel winds (Garreaud 2000).

To display the large-scale patterns of convection and

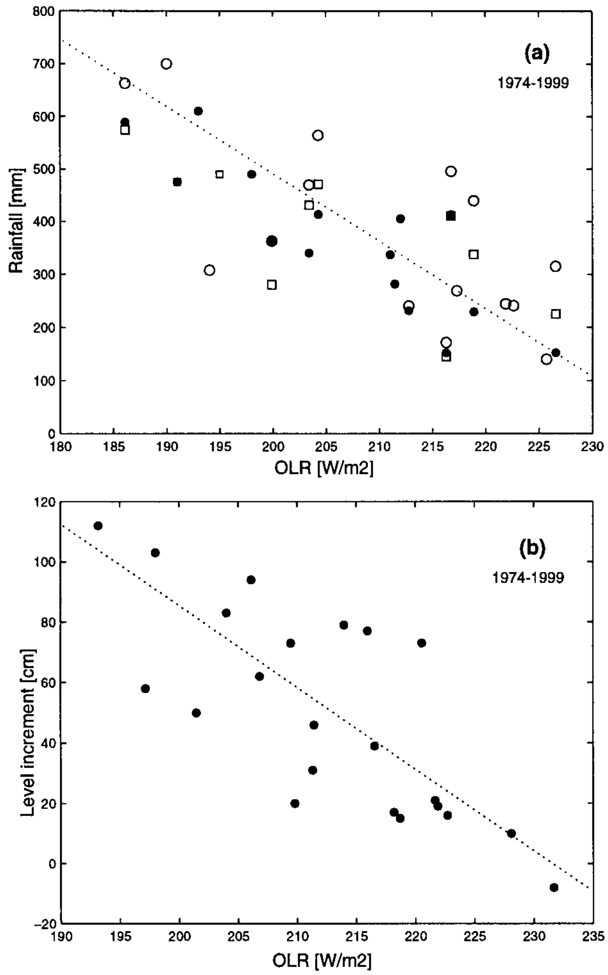

FIG. 3. (a) Scatterplot of the summer rainfall at several stations on the Altiplano and summer mean outgoing longwave radiation (OLR) over the Altiplano (17.5°S, 70°W). The stations are La Paz (16.4°S, 68.2°W, open circles), Oruro (17.9°S, 67°W, filled circles), and Juliaca (15.4°S, 70.3°W, squares). (b) Scatterplot of the summer increment of Lake Titicaca [level at 28 Feb (year 0) minus level at 1 Dec (year −1)] and OLR over the Altiplano (17.5°S, 70°W). Dotted line indicates least square fitting. Analysis periods indicated in each box.

circulation associated with rainfall anomalies over the Altiplano we used 1-point regression maps. The maps display the regression coefficient between a reference time series at one grid box (typically CI) and time series of other gridded variables elsewhere (global fields simultaneous with CI). The regression coefficient $\Re$ is defined at each grid point k as

$$\Re(k) = r(k)\sigma_{F}(k)/\sigma_{RTS}, \quad (1)$$

where $r(k)$ is local correlation coefficient between the time series and the global field, $\sigma_F(k)$ is the standard deviation of the field at this grid point, and σ_{RTS} is the standard deviation of the reference time series. Note that $\sigma_{CI} = 10$ W m^{-2} in the interannual range and $\sigma_{CI} = 20$ W m^{-2} in the intraseasonal range. The numerical value of $\Re$ is indicative of the local anomalies in the field associated with a unit anomaly of the reference time series. The significance of the regression coefficient was assumed to be the same as the correlation coefficient. For this later parameter we used a two-tailed Student's t-test at the 95% confidence level. Wind vector correlations are assumed to be significant if either component is significantly correlated at the 95% confidence level.

Regression maps were produced for intraseasonal and interannual timescales. In the intraseasonal range we used 10 summers (1986–1995) of daily reanalysis and OLR fields. Time series at each grid point were low-pass filtered using a 9-day moving average to eliminate short-lived episodes. For the interannual range we used austral summer (DJF) mean fields of reanalysis and OLR from 1975 to 1999.

3. Overview of intraseasonal variability

Summertime rainy episodes are characterized by high amounts of water vapor in the boundary layer that destabilize the tropospheric column over the Altiplano and give rise to widespread convection along the Plateau (Garreaud 2000). Conversely, during dry periods low-level moisture is very low and convective activity is suppressed or very isolated. Numerical simulations by Garreaud (1999) suggest that moisture fluctuations over the Altiplano are mainly produced by changes in the moisture transport over the eastern slope of the central Andes. On a larger scale, intraseasonal convective anomalies over the Altiplano extend southeastward into southern Bolivia and northern Argentina and tend to be out-of-phase with convective anomalies over the eastern side of the continent and the South Atlantic convergence zone (SACZ; Aceituno and Montecinos 1997; Nogues-Paegle and Mo 1997; Lenters and Cook 1999). This dipolar pattern is evident in the regression map between CI and OLR (Fig. 4a), that also shows significant anomalies over the central equatorial Pacific and the South Pacific convergence zone (SPCZ).

Intraseasonal rainy (dry) episodes are also associated with easterly (westerly) wind anomalies in the middle and upper troposphere over the central Andes (Fuenzalida and Rutllant 1987; Aceituno and Montecinos 1993; Vuille et al. 1998; Lenters and Cook 1999), that, in turn, seem to modulate the regional upslope flow throughout downward momentum flux at the top of the atmospheric boundary layer (Garreaud 1999). As shown in the regression maps between CI and 200 hPa winds and geopotential height (Fig. 4), the westerly (easterly) flow anomalies[2] over the central Andes during periods of suppressed (enhanced) convection are produced by a cyclonic (anticyclonic) anomaly centered over subtropical South America. Superposition of these anomalies on the mean flow is consistent with the intrasea-

[2] The signs of the anomalies in our regression maps are arbitrary but consistent, given the linear character of our analysis.

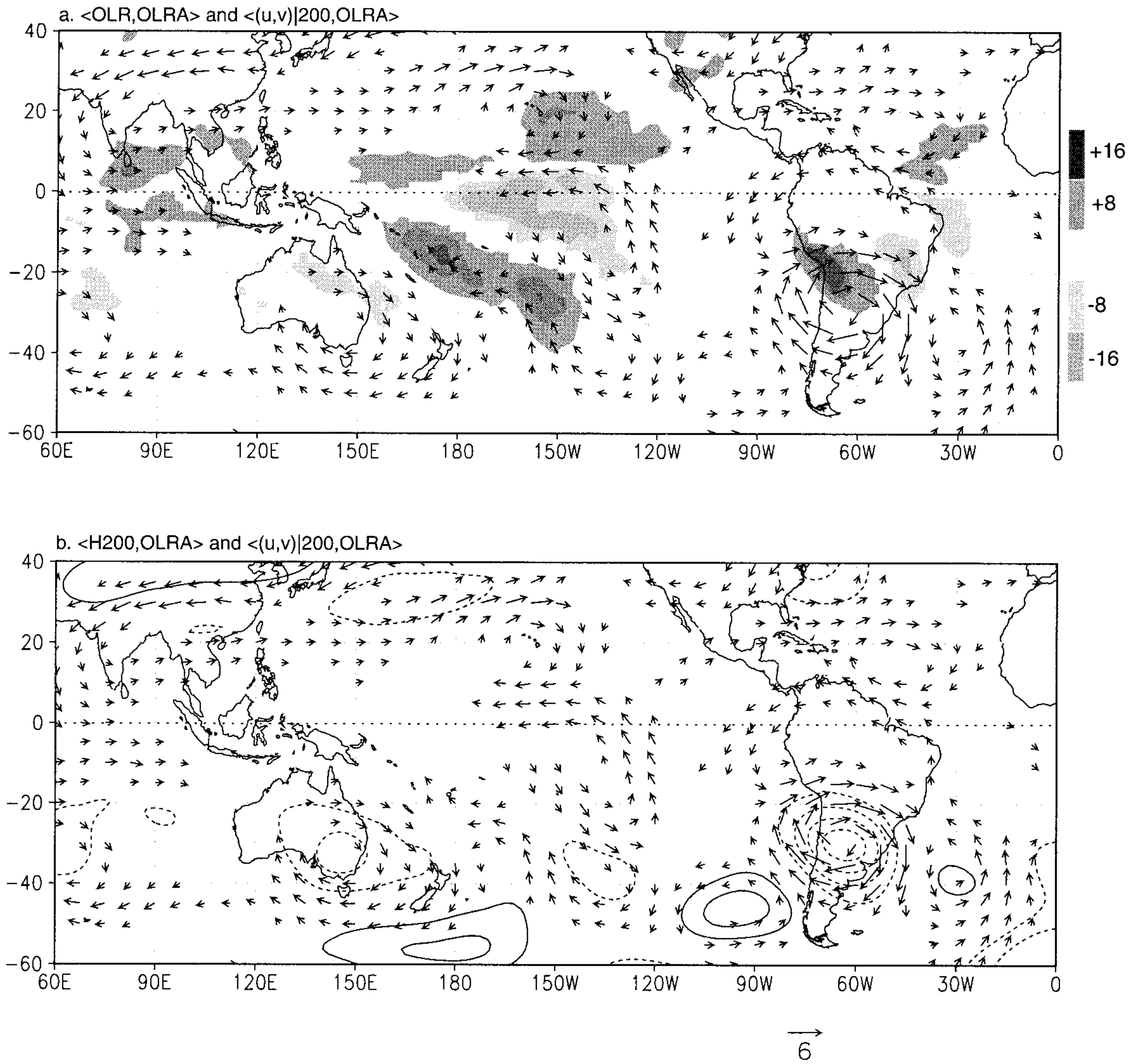

Fig. 4. Regression maps in the intraseasonal range during the austral summer (see section 2 for details on calculation and statistical significance). (a) OLR (shaded, scale in units of W m^{-2} per std dev) and 200-hPa wind regressed upon CI (OLR over the Altiplano). (b) 200-hPa height and winds regressed upon CI. Contour interval is 30 m per std dev. Negative values in dashed line. The zero contour is omitted. Only values and wind vectors statistically significant at the 95% confidence level are shown. Reference wind vector (in m s^{-1}) for both panels at the bottom of the figure.

sonal changes in the position and intensity of the Bolivian high noted in previous studies.

In connection with the circulation anomalies over subtropical South America there is a signature of a wave train over the South Pacific (Fig. 4b). Regression between CI and geopotential height at other pressure levels (not shown) indicates a barotropic character of these extratropical anomalies. Based on similar results for summer (Jones 1990; Nogues-Paegle and Mo 1998; Garreaud 1999) and winter (Mo and Higgins 1997) it has been suggested that intraseasonal circulation anomalies over subtropical South America (and hence, zonal flow anomalies over the central Andes) are likely to be produced by quasi-stationary Rossby waves emanating from the midlatitude south Pacific, and presumably excited by intraseasonal oscillation over the maritime continent.

4. Interannual variability

a. Regression analysis

Figure 5a shows the scatterplot of summer mean 200-hPa zonal wind (UA) and the fraction of days with easterly flow at 200 hPa during the corresponding summer, both at 17.5°S, 70°W. The good fit indicates that summers with mean easterly (westerly) flow have a larger (fewer) number of days with easterly flow.[3] On the

[3] Such relationship could not be expected a priori. One may imagine

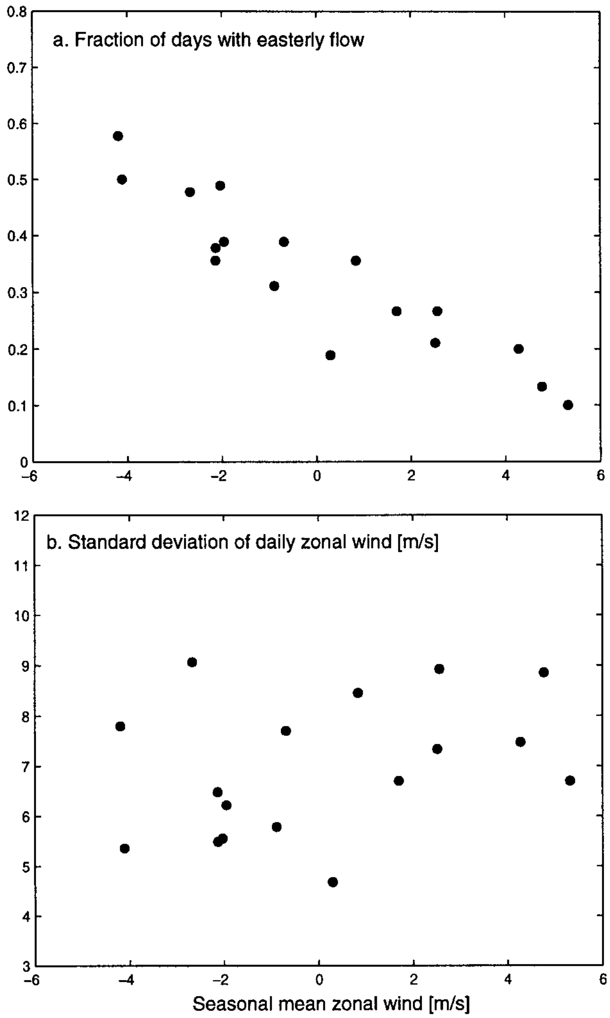

FIG. 5. Scatterplot of intraseasonal 200-hPa zonal wind statistics and austral summer mean 200-hPa zonal flow (UA) over the Altiplano (17.5°S, 70°W). Each summer season comprises 90 days from 1 Dec to 28 Feb. (a) Fraction of summertime days with easterly flow as a function of UA. (b) Std dev of the summer daily mean zonal flow as a function of UA.

other hand, the standard deviation of the daily zonal wind is only weakly dependent on UA (Fig. 5b). Thus, year-to-year differences in the evolution of the zonal wind within the summer occur mainly as a shift in the background level of the flow, without too much change in the amplitude and frequency of intraseasonal fluctuations. Consistently, the time series of daily 200-hPa zonal wind over the Altiplano exhibit intraseasonal fluctuations of similar amplitude and periodicity regardless of the seasonal and monthly means (not shown). Recall from the previous section that intraseasonal fluctuations of the zonal wind over the central Andes are largely produced by extratropical Rossby wave trains amplifying over subtropical South America.

Considering the tight relationship between rainfall and zonal flow during intraseasonal episodes, Fig. 5a also suggests that summers with mean easterly (westerly) flow are associated with rainier (drier) than normal conditions over the Altiplano. This hypothesis is confirmed by the time series of CI and UA shown in Fig. 6 for each summer month. For the whole season, fluctuations of the mean zonal wind explain nearly half of the interannual variance of OLR over the Altiplano ($\sigma \approx 15$ W m^{-2} $\sim$ 150 mm). Note also that the monthly relationship between zonal flow and convection becomes increasingly robust toward the end of the summer season. Such easterly/wet–westerly/dry interannual relationship derived from Fig. 6 was first documented by Kessler (1974) in a comparison of 500-hPa radiosonde winds at Antofagasta (23.5°S, 70.5°W) and the summer increment of Lake Titicaca.

To explore the spatial patterns of the circulation anomalies in the interannual range, Fig. 7 shows the regression maps between seasonal mean CI and OLR, 200-hPa winds and geopotential height. Similar results are found using individual monthly means, as well as summer means in which we have excluded the summer of 1982(D)/83(JF), the strongest El Niño in our records. Convection anomalies with the same sign of those over the Altiplano are found along the central and equatorial Andes, extending from the northeastern side of the continent into the tropical Atlantic, while out-of-phase anomalies prevail over the SACZ root region. The lack of convection anomalies over the Amazon basin is consistent with the relatively weak interannual fluctuations in this region (e.g., Liebmann et al. 1999). Overall, the Altiplano-related interannual pattern of OLR over South America is similar to the pattern in the intraseasonal range (cf. Figs. 4a and 7a).

The zonal wind anomalies upstream and downstream of the central–tropical Andes are consistent with the easterly/wet–westerly/dry relationship derived for the Altiplano and the results obtained by Vuille (1999) using a compositing analysis. The circulation pattern is largely a tropical feature, in contrast with the subtropical–extratropical pattern that emerges in the intraseasonal range (cf. Figs. 4b and 7b), with wind anomalies in geostrophic balance with changes in the meridional baroclinicity between tropical and subtropical latitudes. Furthermore, an almost identical circulation pattern emerges from the regression of the 200-hPa wind upon UA (not shown), suggesting that this pattern is not only related to rainfall anomalies on the Altiplano but it is also the *internal* leading mode of interannual zonal flow variability over the central Andes.

Significant anomalies of OLR and 200-hPa circulation related to CI variability are also found over the rest of the Tropics. Overall, they bear strong resemblance to ENSO-related anomalies (e.g., Yulaeva and Wallace

---

for instance, a year in which weak easterly wind prevail during most of the time, but a few days with strong westerly winds produce a westerly seasonal mean.

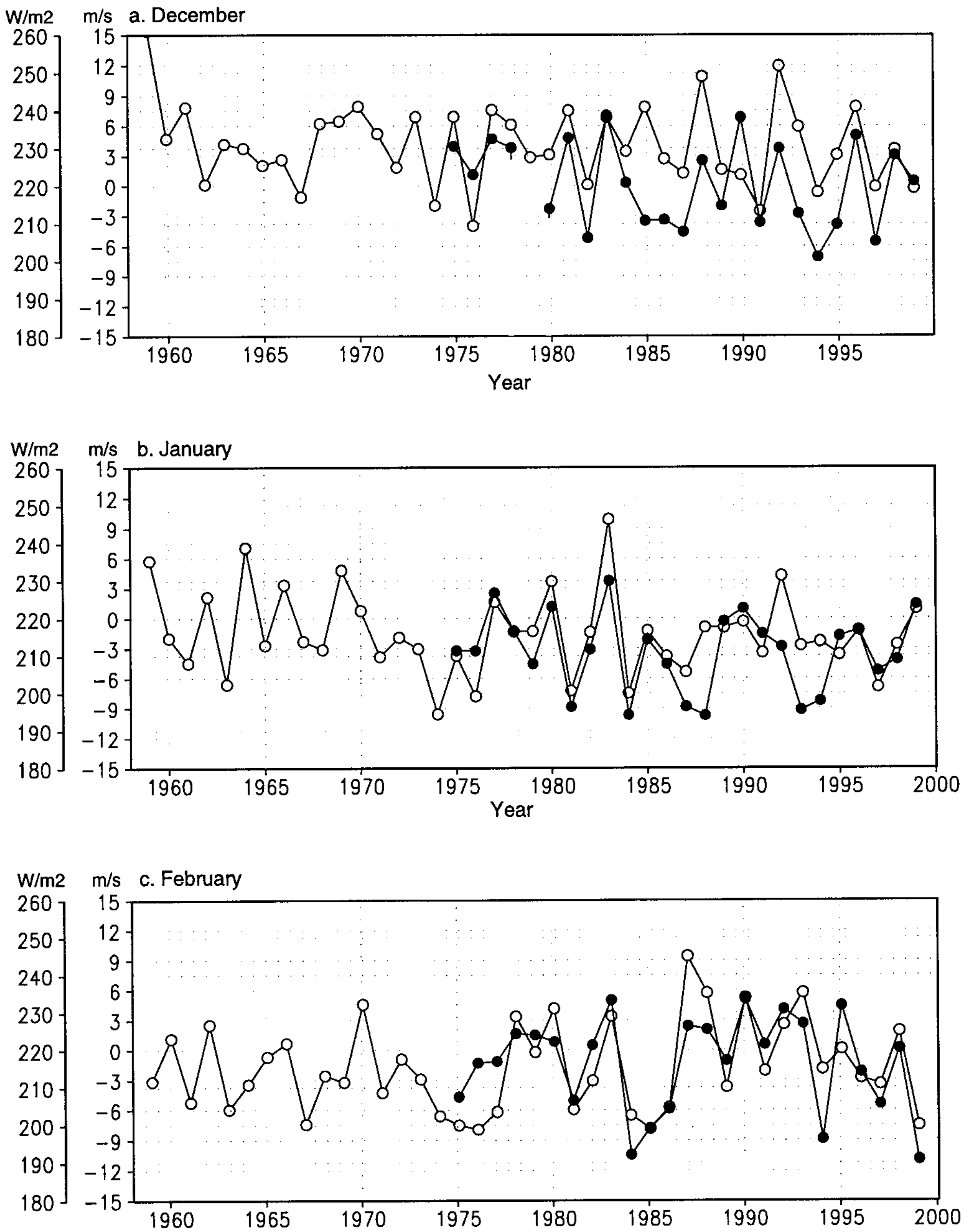

FIG. 6. Monthly mean values of zonal wind at 200 hPa (open circles) and OLR (closed circles) over the Altiplano (17.5°S, 70°W) for each summer month.

1994). For instance, dry conditions over the Altiplano are associated with upper-level westerly anomalies over much of the central Pacific (weakened Walker cell) and a dipole in convective cloudiness over the western tropical Pacific typical of El Niño events. The 200-hPa geopotential height pattern for this case (Fig. 7b) is also consistent with the generalized warming of the tropical troposphere during the warm ENSO phase, including the distinctive twin peaks flanking the region of enhanced convection over the central Pacific (Yulaeva and Wallace 1994).

b. Discussion

The previous results suggest that the association between El Niño (La Niña) and drier (rainier) than normal summers on the Altiplano can be explained by ENSO-related warming (cooling) of the tropical troposphere, especially over tropical South America and the eastern Pacific, upon which intraseasonal episodes are superimposed. Interannual variability of the tropical troposphere temperature is also responsible for ENSO-related summertime rainfall anomalies along the eastern side of

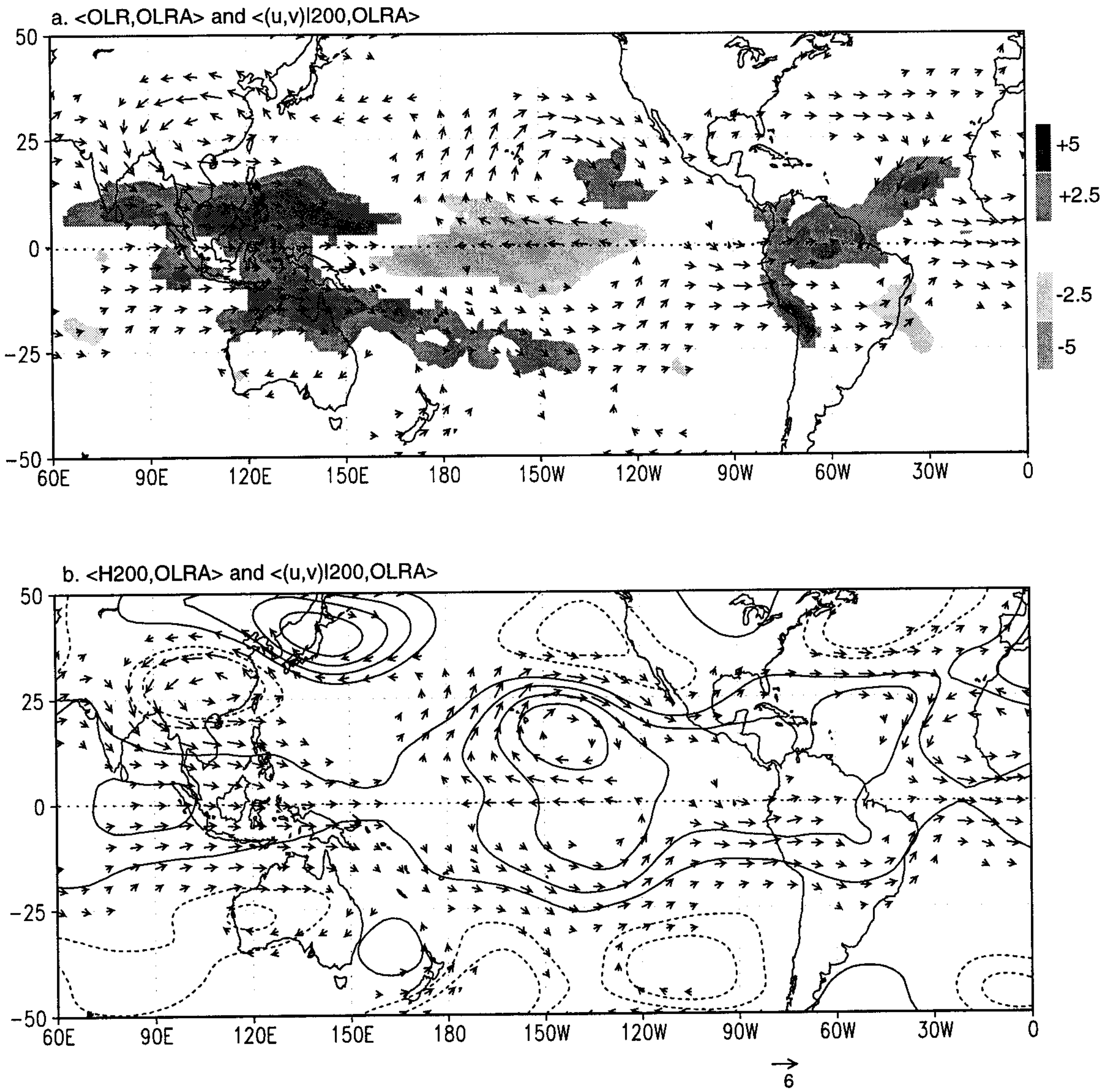

FIG. 7. Regression maps in the interannual range (see section 2 for details on calculation and statistical significance). (a) OLR (shaded, scale in units of W m^{-2} per std dev) and 200-hPa wind regressed upon CI (OLR over the Altiplano). (b) 200-hPa height and winds regressed upon CI. Contour interval is 30 m per std dev. Negative values in dashed line. The zero contour is omitted. Only values and wind vectors statistically significant at the 95% confidence level are shown. Reference wind vector (in m s^{-1}) at the bottom of the figure.

subtropical South America. For instance, while the enhanced subtropical jet stream (westerly flow) during El Niño years tends to suppress convection over the Altiplano it also favors the maintenance of persistent frontal activity in southern Brazil (e.g., Kousky et al. 1984; Lenters and Cook 1999). In between these coherent but opposite signals, rainfall anomalies over the Bolivian lowlands to the east of the Andes are largely independent of ENSO (Ronchail 1998). ENSO-related warming or cooling of the tropical troposphere also explains a strong, direct relationship between ENSO phases and the low-level temperature anomalies over the Altiplano, as documented in Vuille (1999) and Vuille et al. (2000).

Given the marked similarity between circulation anomalies associated with Altiplano rainfall variability and the canonical ENSO signal, one may wonder why the ENSO–Altiplano rainfall relationship is rather weak. To understand this paradox we examine 200-hPa wind and geopotential anomalies (full field minus climatology) for 2 months when the relationship does not hold (Fig. 8). Our first example is January 1973, during the mature stage of a moderate El Niño (SOI = −0.5) and Altiplano rainfall slightly *above* normal. Tropospheric warming over the tropical eastern Pacific and South America is evident during this month (positive 200-hPa height anomalies, Fig. 8a). However, the anomalous warming extended well into the subtropics so that the increase in upper-level zonal wind take places between

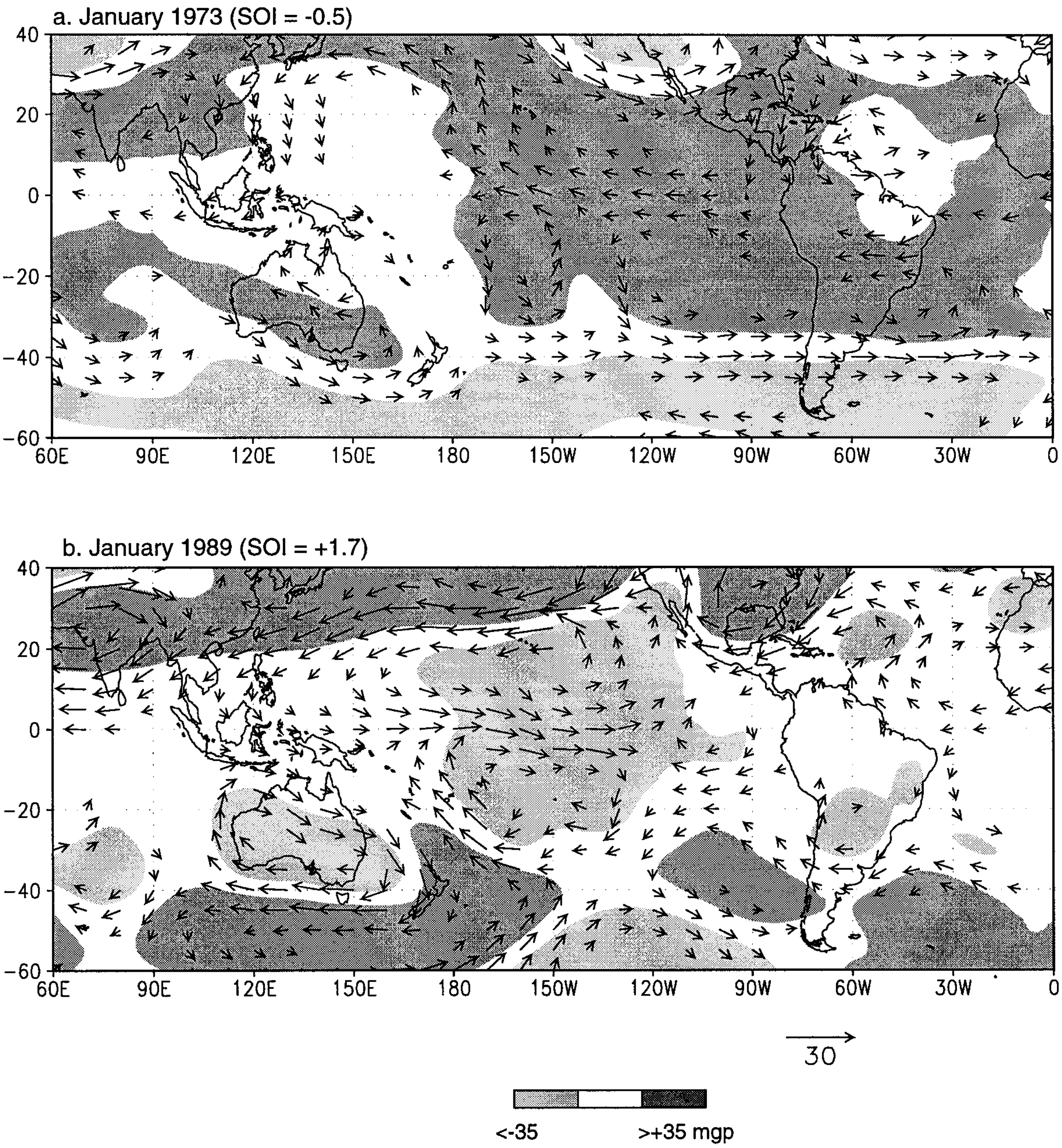

FIG. 8. 200-hPa wind anomalies (vectors; reference at the bottom in m s^{-1}) and geopotential height anomalies (shaded) during Jan 1973 (El Niño conditions with above normal Altiplano rainfall). Anomalies calculated as departure from the climatological summer mean (1958–99). Only wind anomalies in excess of 5 m s^{-1} are shown. (b) As (a) but for Jan 1989 (La Niña conditions with below normal Altiplano rainfall).

30° and 40°S, leaving the central Andes under near-climatological flow. Our second example is January 1989, during the mature stage of La Niña (SOI = +1.7) and Altiplano rainfall well *below* than normal. As expected, anomalous cooling is found over the central Pacific and much of the Tropics. In this case, however, there is also a region of significant cooling to the southeast of the central Andes leading to southerly wind anomalies over the Altiplano (Fig. 8b).

Thus, even though the large-scale pattern during individual months (or seasons) looks similar to the canonical ENSO signal, rainfall anomalies on the Altiplano are highly dependent upon the position, intensity and timing of anomalous meridional baroclinicity. The relatively weak statistical relationship between interannual variability of basin-averaged rainfall and ENSO indices (e.g., SOI) can also be produced by the high spatial rainfall variability over the Altiplano (Vuille et al. 2000).

Generalized warming/cooling of the tropical troposphere could be produced by phenomena other than ENSO. Of particular relevance on interannual or longer timescales is the Pacific decadal oscillation since it features tropical signatures similar to those associated with ENSO (Zhang et al. 1997; Garreaud and Battisti 1999). The ''warm'' conditions over the central equatorial Pacific during the late 70s and 80s are thus consistent with drier than normal conditions observed on the Altiplano during that period (Vuille et al. 2000).

5. Concluding remarks

The relationship between interannual variability of the large-scale circulation and the Altiplano (area-averaged) summer rainfall has been investigated in this work on the basis of an observational analysis. One must keep in mind, however, that the strength of such relationship varies across the basin, and that validity of our results should be confirmed by numerical experiments using global climate models. Thus far, our main findings are as follows.

- Interannual fluctuations in rainfall on the Altiplano, extending along the central and equatorial Andes, and upper-level zonal wind anomalies over the western side of tropical South America and the eastern Pacific exhibit a easterly/wet–westerly/dry relationship. The circulation anomalies are in geostrophic balance with changes in the meridional baroclinicity caused by temperature anomalies of the tropical troposphere.
- The amplitude and frequency of intraseasonal zonal flow fluctuations (forced from the SH extratropics) are largely independent of the mean tropical conditions. Thus, superposition of intraseasonal variability and the seasonal mean conditions results in summertime fluctuations of the number of days with easterly wind over the Altiplano that are consistent with the seasonal mean flow. Given the tight correspondence between rainfall and zonal flow during intraseasonal episodes, the following chain is proposed for summertime interannual variability:

$$\text{seasonal mean} \begin{pmatrix} \text{easterly} \\ \text{westerly} \end{pmatrix} \text{flow}$$

$$\rightarrow \begin{pmatrix} + \\ - \end{pmatrix} \text{days with easterly flow}$$

$$\rightarrow \begin{pmatrix} + \\ - \end{pmatrix} \text{days with precipitation}$$

- The previously documented relationship between ENSO and Altiplano interannual rainfall anomalies can be explained by the generalized warming (cooling) of the tropical troposphere during the warm (cold phase) of ENSO, and the associated changes in the seasonal mean zonal flow aloft at tropical-subtropical latitudes. The amount (and even the sign) of the Altiplano rainfall anomalies is, however, highly dependent on the location of zonal wind anomalies. Thus, seasonal prediction in this region requires detailed knowledge of the structure of the tropical-subtropical tropospheric temperature anomalies.

Acknowledgments. NCAR–NCEP reanalysis and OLR data were provided by the NOAA Climate Diagnostics Center. The authors gratefully acknowledge Mathias Vuille, David Thompson, and Todd Mitchell for comments and a careful reading of this manuscript. The comments of Dr. Kerry Cook and an anonymous reviewer led to substantial improvements in the presentation and content of this paper.

REFERENCES

Aceituno, P., 1988: On the functioning of the Southern Oscillation in the South American sector. Part I: Surface climate. *Mon. Wea. Rev.,* **116,** 505–524.

——, 1998: Climate elements of the South American Altiplano (in Spanish). *Rev. Geofisica-IPGH,* **44,** 37–55.

——, and A. Montecinos, 1993: Circulation anomalies associated with dry and wet periods in the South American Altiplano. *Proc. Fourth Int. Conf. on Southern Hemisphere Meteorology,* Hobart, Australia, Amer. Meteor. Soc., 330–331.

——, and R. D. Garreaud, 1995: The impact of the ENSO phenomenon in the rainfall regime along the Andes cordillera (in Spanish). *Rev. Chilena Ing. Hidraulica,* **2,** 33–43.

——, and A. Montecinos, 1997: Patterns of convective cloudiness in South America during austral summer from OLR pentads. Preprints, *Fifth Int. Conf. on Southern Hemisphere Meteorology and Oceanography,* Pretoria, South Africa, Amer. Meteor. Soc., 328–329.

——, and ——, 2000: Diurnal cycle over the South American Altiplano: Comparison between NCEP/NCAR reanalysis with upper-air observations during the *Visviri* field experiments. Preprints, *Sixth Int. Conf. on Southern Hemisphere Meteorology and Oceanography,* Santiago, Chile, Amer. Meteor. Soc., 412–413.

Dai, A., I. Y. Fung, and A. D. Del Genio, 1997: Surface observed global land precipitation variations during 1900–1988. *J. Climate,* **10,** 2943–2962.

Francou, B., and L. Pizarro, 1985: El Niño y la sequía en los Altos Andes centrales (Perú y Bolivia). *Bull. Inst. Francais Études Andines,* **14,** 1–18.

Fuenzalida, H., and J. Rutllant, 1987: Origen del vapor de agua que precipita sobre el altiplano de Chile. Proc. *II Congreso InterAmericano de Meteorología,* Buenos Aires, Argentina, 6.3.1–6.3.4.

Garreaud, R. D., 1999: A multiscale analysis of the summertime precipitation over the central Andes. *Mon. Wea. Rev.,* **127,** 901–921.

——, 2000: Intraseasonal variability of moisture and rainfall over the South American Altiplano. *Mon. Wea. Rev.,* **128,** 3379–3346.

——, and D. S. Battisti, 1999: Interannual (ENSO) and interdecadal (ENSO-like) variability in the Southern Hemisphere tropospheric circulation. *J. Climate,* **12,** 2113–2123.

Hulme, M., 1992: A 1951–80 global land precipitation climatology for the evaluation of general circulation models. *Climate Dyn.,* **7,** 57–72.

Jones, C., 1990: An investigation of low-frequency variability of the large-scale circulation over South America. M.S. thesis, Meteorology Department, University of Utah, 103 pp. [Available from Meteorology Department, University of Utah, Salt Lake City, UT 84112-0110.]

Kalnay, E., and Coauthors, 1996: The NCEP/NCAR 40-Year Reanalysis Project. *Bull. Amer. Meteor. Soc.,* **77,** 437–471.

Kessler, A., 1974: Atmospheric circulation anomalies and level fluctuations of Lake Titicaca. *Bonner Meteor. Abh.,* **17,** 361–372.

Kousky, V. E., M. T. Kagano, and I. F. Cavalcanti, 1984: A review of the Southern Oscillation: Oceanic–atmospheric circulation changes and related rainfall anomalies. *Tellus,* **36a,** 490–504.

Lenters, J. D., and K. H. Cook, 1999: Summertime precipitation variability over South America: Role of the large-scale circulation. *Mon. Wea. Rev.,* **127,** 409–431.

Liebmann, B., and C. A. Smith, 1996: Description of a complete (interpolated) outgoing longwave radiation dataset. *Bull. Amer. Meteor. Soc.,* **77,** 1275–1277.

——, G. Kiladis, J. Marengo, T. Ambrizzi, and J. Glick, 1999: Submonthly convective variability over South America and the South Atlantic Convergence Zone. *J. Climate,* **11,** 2898–2909.

Meisner, B., and P. Arkin, 1987: Spatial and annual variations in the diurnal cycle of the large-scale tropical convective cloudiness and precipitation. *Mon. Wea. Rev.,* **115,** 2009–2032.

Mo, K. C., and R. W. Higgins, 1997: The Pacific–South American mode and tropical convection during the Southern Hemisphere winter. *Mon. Wea. Rev.,* **126,** 1581–1596.

Nogues-Paegle, J., and K. C. Mo, 1997: Alternating wet and dry conditions over South America during summer. *Mon. Wea. Rev.,* **125,** 279–291.

Ronchail, J., 1995: Variabilidad interanual de las precipitaciones en Bolivia. *Bull. Inst. Francais Études Andines,* **24,** 369–378.

——, 1998: Variabilité Pluviométrique en Bolivie lors des phases extrémes de l' Oscillation Australe du Pacifique (1950–93). *Bull. Inst. Francais Études Andines,* **27,** 687–698.

Schwerdtfeger, W., 1976: High thunderstorm frequency over the subtropical Andes during summer: Cause and effects. *Climate of Central and South America,* W. Schwerdtfeger, Ed., Elsevier, 192–195.

Thompson, L. G., E. Mosley-Thompson, and B. J. Morales Arnao, 1984: El Niño–Southern Oscillation events recorded in the stratigraphy of the tropical Quelccaya ice cap, Peru. *Science,* **226,** 50–52.

——, and Coauthors, 1998: A 25 000 year tropical climate history from Bolivian ice cores. *Science,* **282,** 1858–1864.

Vuille, M., 1999: Atmospheric circulation over the Bolivian Altiplano during dry and wet periods and extreme phases of the Southern Oscillation. *Int. J. Climatol.,* **19,** 1579–1600.

——, D. R. Hardy, C. Braun, F. Keimig, and R. S. Bradley, 1998: Atmospheric circulation anomalies associated with 1996/97 summer precipitation events on Sajama Ice Cap, Bolivia. *J. Geophys. Res.,* **103,** 11.191–11.204.

——, R. S. Bradley, and F. Keimig, 2000: Interannual climate variability in the central Andes and its relation to tropical Pacific and Atlantic forcing. *J. Geophys. Res.,* **105,** 12 447–12 460.

Yulaeva, E., and J. M. Wallace, 1994: The signature ENSO in global temperature and precipitation fields derived from the Microwave Sounding Unit. *J. Climate,* **7,** 1719–1736.

Zhang, Y., J. M. Wallace, and D. S. Battisti, 1997: ENSO-like interdecadal variability: 1900–1993. *J. Climate,* **10,** 1004–1020.

Zhou, J., and K. M. Lau, 1998: Does a monsoon climate exist over South America? *J. Climate,* **11,** 1020–1040.